

## Possible Biological Activity in Proton, Metal, and Aminohydroxamic Acid Equilibria. Protonation and Complex Formation Reactions between *N*-Hydroxy-D-asparagine and Cobalt(II), Nickel(II), Copper(II), and Hydrogen Ions in Aqueous Solution

Enrico Leporati

*Istituto di Chimica Generale ed Inorganica dell'Universita' degli Studi di Parma, Viale delle Scienze, 43100 Parma, Italy*

The protonation and complex-formation equilibria in aqueous solutions between  $H^+$ ,  $Co^{II}$ ,  $Ni^{II}$ , and  $Cu^{II}$  and *N*-hydroxy-D-asparagine (hasn) have been investigated by the potentiometric method in 0.5 mol dm<sup>-3</sup> KCl solution at 25 °C. The specific tendencies of aminohydroxamic acids towards different metal ions have been tested as models for substratum-metal bonding in biological reactions. The following overall formation constants  $\beta_{pqr} = [M_p H_q L_r] / [M]^p [H]^q [L]^r$  were obtained: hasn,  $\log \beta_{011} = 9.37(1)$ ,  $\log \beta_{021} = 17.52(1)$ ,  $\log \beta_{031} = 19.70(1)$ ;  $Co^{II}$ -hasn,  $\log \beta_{111} = 13.91(2)$ ,  $\log \beta_{101} = 7.56(2)$ ,  $\log \beta_{203} = 23.43(3)$ ,  $\log \beta_{102} = 12.86(3)$ ,  $\log \beta_{1-12} = 2.46(7)$ ;  $Ni^{II}$ -hasn,  $\log \beta_{111} = 14.25(3)$ ,  $\log \beta_{101} = 8.38(3)$ ,  $\log \beta_{102} = 14.73(6)$ ,  $\log \beta_{203} = 25.78(4)$ ;  $Cu^{II}$ -hasn,  $\log \beta_{101} = 12.60(1)$ ,  $\log \beta_{203} = 37.45(5)$ ,  $\log \beta_{304} = 53.43(9)$ ,  $\log \beta_{102} = 19.07(4)$ ,  $\log \beta_{1-12} = 9.08(4)$ . The ligands are bound to the metals through the *N* atom of the  $\alpha$ -amino group, and by the deprotonated  $NHO^-$  group *via* the *N* or *O* atom. Electronic spectra under the same experimental conditions have been recorded and discussed. They provide important evidence for the formation of different metal complexes of *N*-hydroxy-D-asparagine, depending on the pH and can also be used to estimate the co-ordination sphere around the metal ions and to observe the equilibria between different complexes.

Following research on the protonation and complex-formation equilibria of aminohydroxamic acids, a potentiometric study of *N*-hydroxy-D-asparagine (hasn),  $HOOC-CH(NH_2)-CH_2CO-NHOH$ , has been undertaken. Hydroxamic and aminohydroxamic acids and their metal chelates were found to play an important role in living systems as therapeutic substances in the treatment of hepatic coma,<sup>1</sup> constituents of antibiotics, urease activity and tumour inhibitors,<sup>2</sup> pigments and cell division<sup>3,4</sup> growth factors. These effects are intimately connected with iron transport phenomena in the metabolism of micro-organisms.<sup>5,6</sup> Apart from porphyrins, hydroxamic acids are the other major class of naturally occurring iron complexing agents. While  $Fe^{III}$ -hydroxamate complexes are very stable, the corresponding  $Fe^{II}$  complexes are relatively unstable. This is incompatible with an oxidation-reduction mechanism for the iron but is, on the other hand, ideally suited for the biological role the hydroxamate is supposed to play, *i.e.* metal transport. In addition there is an important biochemical interest in the hydroxamic acids, as a result of finding the oxidized peptide group,  $-CON(OH)-$ , in a number of natural products, especially in antibiotics and bacterial growth factors. In the same way hydroxamic acids reveal a number of pharmacological actions including antituberculous, antifungus, and antileukaemic activities.<sup>7,8</sup> Moreover some hydroxamic acids can be employed as indicators of biological activity with the eventual purpose of designing metal chelates as suitable sources of various trace elements essential in animal nutrition. Although the mechanism of their chemical action is not known, there is reason to suspect that the interaction of this ligand with metal ions holds a particular meaning. *X*-Ray crystallographic studies of  $[NiL_2]$  ( $HL = 2$ -amino-*N*-hydroxyacetamide) have been made recently by Pakkanen and co-workers.<sup>9</sup>

As discussed previously,<sup>10</sup> the rate of transfer of iron from a chelate to apotransferrin *via* an intermediate ternary complex<sup>11</sup> may be a critical factor in determining the efficacy of a given

iron chelate as an oral source of iron. It has also been pointed out recently that aminohydroxamic acids may be particularly active because of a possible surface-active role by an unco-ordinated amino group;<sup>12</sup> however, in the case of  $Co^{II}$ ,  $Ni^{II}$ , and  $Cu^{II}$  complexes of 2-amino-*N*-hydroxyacetamide (aha) and 2-amino-*N*-hydroxypentanamide (ahp), I have shown recently<sup>13</sup> that co-ordination clearly involves not only the deprotonated  $NHO^-$  group but also the amino group. In spite of the great interest in the solution chemistry of hydroxamic acids and metal hydroxamates and their biological role, studies on aminohydroxamic acids and their metal complexes are scarce. The hydroxamic acid moiety as a typical bidentate donor behaves very much like acetylacetone towards different metal ions.<sup>13,14</sup> However, in the presence of another donor group in the same molecule, the hydroxamate group has been shown to behave in a monodentate manner, co-ordination to  $Cu^{II}$  and  $Ni^{II}$  taking place through its nitrogen atom, after an induced deprotonation takes place.<sup>15</sup> However, in the field of analytical chemistry hydroxamic acids have long had a role that is independent of their function as iron transport agents for micro-organisms. These ligands have found widespread use as analytical reagents for a variety of metal ions.<sup>16</sup> Yet in spite of their extensive analytical applications, few detailed potentiometric studies have been made of the metal complexes that are formed. In this paper I report results concerning the potentiometric behaviour of bidentate *N*-hydroxy-D-asparagine, alone and in the presence of metal ions in aqueous solution, and extend the studies on the visible spectra of the same solutions.

### Experimental

**Reagents.**—*N*-Hydroxy-D-asparagine (hasn) was obtained from Sigma (St. Louis) and its purity checked potentiometrically. Doubly distilled and deionized water was used throughout and all potentiometric experiments were carried out under an atmosphere of purified nitrogen. Concentrations of stock

solutions of bivalent metal chlorides (AnalaR products) were determined by inductively coupled plasma (i.c.p.) atomic emission spectrometry. All other chemicals employed were of the highest grade available and were prepared and purified by the methods described previously.<sup>17-20</sup> High purity potassium chloride (Merck) was used as supporting electrolyte and the ionic medium was 0.5 mol dm<sup>-3</sup> KCl at the beginning of each potentiometric titration. The starting solutions for each potentiometric experiment were obtained by adding successively to the titration compartment a known volume of hasn solution, and an exact volume of metal chloride; then the required quantities of potassium chloride (Merck), used as supporting electrolyte in order to minimize variations of the activity coefficients in spite of wide changes in the concentration of the reagents, and a sufficient amount of doubly distilled water were added to make up the total volume  $V_0$ , which was 25.0 ± 0.015 cm<sup>3</sup>. Carbonate-free potassium hydroxide solution was prepared and standardized by potentiometric titration of a known amount (*ca.* 2.0 cm<sup>3</sup>) of hydrochloric acid (0.2969 mol dm<sup>-3</sup>) as previously described.<sup>13,18,19</sup>

**Potentiometric Measurements.**—Potentiometric titrations were performed using a Metrohm Titroprocessor E 636, equipped with an H 268 glass electrode (Schott-Jena glass) and a B 343 Talamid reference electrode (Schott-Jena glass). The electrode system was calibrated by periodic dynamic titrations of hydrochloric acid (*ca.* 2.0 cm<sup>3</sup>, 0.2969 mol dm<sup>-3</sup>) in 0.5 mol dm<sup>-3</sup> KCl at 25 °C with standard potassium hydroxide solution. The resulting titration data were used to calculate the standard electrode potential ( $E^\circ$ ), the coefficients of the correction terms for the effects of both liquid-junction potential in acid ( $A_j$ ) and basic ( $B_j$ ) solution, the equivalence point ( $v_e$ ), the concentration of the standard potassium hydroxide solution ( $N$ ), and the dissociation constant of water ( $K_w$ ), following the calculation procedures described previously.<sup>12,18,21,22</sup> The solution in the titration vessel was stirred by means of a mechanical stirrer. A stream of nitrogen, presaturated with water vapour by bubbling it through a thermostatted 0.5 mol dm<sup>-3</sup> KCl solution, was blown over the surface of the solution. All the alkalimetric titrations were carried out at 25.0 ± 0.1 °C and  $I = 0.5$  mol dm<sup>-3</sup> (KCl) as previously reported<sup>15-17</sup> for solutions of binary systems containing copper(II), nickel(II), cobalt(II), and/or ligand (hasn) at different molar ratios. E.m.f. readings and titration curves were recorded graphically by using a E 636 automatic titrator equipped with a thermoprinter. Small amounts (0.05 cm<sup>3</sup>) of titrant (KOH) were added with the use of a Metrohm Dosimat E 635 autoburette (total volume 5.0 cm<sup>3</sup>). The collection of experimental data ( $v$ ,  $E$ ) was performed by using two different methods: 'kinetics D' or 'kinetics T'. The 'kinetics' parameter determines the moment at which the e.m.f. value ( $E$ ) is recorded in the computer memory. It is possible to choose the measurement manner 'D' (control of the drift) and the system 'T' (time of constant wait), while the e.m.f. value is defined in each case by the typical quantity 'kinetics'. For the 'kinetics D' it is possible to choose the values of drift from 0.5 to 75 mV min<sup>-1</sup>, subdivided in 10 steps. At fixed intervals, an e.m.f. measurement is performed by calculating its variation with reference to the last measurement and by comparing it with the selected limit value. If the drift of the signal is too great, another measurement can be effected and this process is repeated until it is possible to obtain a result which can be stored in the memory. The 'waiting time' owing to the drift has a lower limit of about 2 s and an upper limit of about 60 s. In the 'kinetics T' method the e.m.f. values are stored after a constant waiting time of 2 300 s, regulable in 10 steps. This allows, under the chosen experimental conditions, amelioration of measurement repetition especially in the case of a very slow response or reaction (*e.g.* titration in non-aqueous solution).

**Spectrophotometric Measurements.**—Absorption spectra in the region 440–800 ± 1 nm were recorded on a Jasco Uvidec-505 spectrophotometer, equipped with a DP-101 digital printer. Matched quartz cells of pathlength 1.0 cm, calibrated before use, were employed. Measurements of potential were achieved with the system used in the potentiometric titrations, calibrated in the same way. Samples containing hasn and copper ion maintained at an ionic strength of 0.5 mol dm<sup>-3</sup> KCl and at 25 °C were scanned at pH values from 3.30 to 11.42 using 10-mm cells.

**Calculation Methods.**—Great care has been paid to the calculation procedures and critical evaluation of some parameters pertaining to potentiometric calibration curves, using different mathematical methods. In the potentiometric titrations  $E^\circ$ ,  $A_j$ ,  $B_j$ ,  $N$ ,  $K_w$ , and  $v_e$  were calculated under the same experimental conditions, according to Gran's procedure<sup>22,23</sup> and a pseudo-Nernstian behaviour, equations (1a) and (1b). The overall stability constants ( $\beta_{par}$ ) were refined by

$$E = E^\circ + \frac{RT}{F} \ln[H^+] + A_j [H^+] \quad (\text{acid solution}) \quad (1a)$$

$$E = E^\circ + \frac{RT}{F} \ln[OH^-] + \frac{RT}{F} \ln K_w + B_j \frac{K_w}{[H^+]} \quad (\text{basic solution}) \quad (1b)$$

rigorous least squares using the computer program SUPERQUAD;<sup>24</sup>  $p, q$  and  $r$  are the stoichiometric coefficients of metal(II), proton, and ligand, respectively, in the complex  $M_p H_q L_r$ . This program calculates the values of the cumulative protonation and formation constants which minimize the weighted sum ( $U$ ) of the squared residuals between observed and calculated e.m.f. values, equation (2). The parameter  $Z$  is the

$$U = \sum_{i=1}^Z w_i (E_i^{\text{obs.}} - E_i^{\text{calc.}})^2 \quad (2)$$

total number of potentiometric data (e.m.f.) and  $w_i$  is the weighting factor, defined by equation (3) and assigned to the  $i$ th

$$w_i = 1/[\sigma_E^2 + (\partial E_i / \partial v_i)^2 \sigma_v^2] \quad (3)$$

observation, where  $\sigma_E (=0.2)$  is the error in the e.m.f. and  $\sigma_v (=0.008)$  the error in the volume used in the refinement.

For protonation equilibria the computer program GAUSS Z<sup>25</sup> was also applied. This computes the values of the overall protonation or formation constants which minimize the unweighted sum of the squared residuals between observed and calculated protonation functions,  $\bar{n}$ , equation (4), where  $\bar{n}$  is the

$$U^H = \sum_{i=1}^Z (\bar{n}_i^{\text{calc.}} - \bar{n}_i^{\text{obs.}})^2 \quad (4)$$

total concentration of hydrogen ion bound to the ligand divided by the total concentration of the ligand, or the average number of hydrogens bound to each central ligand molecule. At first the cumulative protonation constants of the ligand were determined separately by GAUSS Z and SUPERQUAD through the refinement of several sets of potentiometric data; the values obtained were introduced as constants into the SUPERQUAD refinement process of the complex formation constants for binary systems. All the calculations were carried out on the CRAY X-MP/12 and IBM 4341/10 computers of the Consorzio per la Gestione del Centro di Calcolo Elettronico Inter-universitario dell'Italia Nord Orientale, Casalecchio, Bologna,

**Table 1.** Summary of titration data used in formation constant calculations. Initial amounts of the reagents\* for the potentiometric titrations of *N*-hydroxy-D-asparagine (hasn) with bivalent metal ions at 25°C and  $I = 0.5 \text{ mol dm}^{-3}$  (KCl)

Run	System	$T_L$	$T_M$	$T_H$	pH range
1	H <sup>+</sup> -hasn	0.259 89		0.792 79	2.24—10.91
2		0.227 41		0.693 69	2.28—11.22
3		0.194 92		0.594 59	2.38—11.11
4		0.246 90		0.753 15	2.26—10.97
5		0.272 88		0.832 43	2.28—11.31
6	Cu <sup>II</sup> -hasn	0.232 67	0.051 61	0.694 58	2.37—10.30
7		0.232 67	0.083 33	0.694 58	2.36—10.31
8		0.199 43	0.102 96	0.595 36	2.44—11.27
9		0.265 91	0.101 71	0.793 81	2.30—10.26
10		0.252 61	0.066 86	0.754 12	2.33—9.82
11	Ni <sup>II</sup> -hasn	0.232 67	0.058 80	0.694 58	2.34—10.87
12		0.232 67	0.117 61	0.694 58	2.33—8.02
13		0.199 43	0.147 01	0.595 36	2.40—6.80
14		0.212 73	0.073 50	0.635 05	2.37—10.92
15		0.252 61	0.066 15	0.754 12	2.35—11.01
16		0.265 91	0.147 01	0.793 81	2.29—7.72
17	Co <sup>II</sup> -hasn	0.226 02	0.062 40	0.674 74	2.36—9.51
18		0.226 02	0.112 88	0.674 74	2.35—10.85
19		0.259 26	0.138 80	0.773 97	2.31—8.17
20		0.299 14	0.105 15	0.893 04	2.30—9.42
21		0.285 85	0.067 42	0.853 35	2.28—9.20
22		0.319 09	0.130 96	0.952 57	2.25—10.70

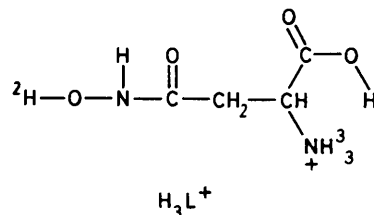
\*  $T_L$  = mmol of ligand,  $T_M$  = mmol of metal,  $T_H$  = mmol of hydrogen in the titration vessel.

with financial support from the University of Parma. The compositions of the starting solutions for each potentiometric titration are reported in Table 1. Listings of experimental data and final computations from SUPERQUAD and GAUSS Z are available on request from the author.

## Results and Discussion

**Protonation Equilibria.**—Initially the cumulative protonation constants of the ligand and the initial amounts (mmol) of reagents ( $T_L, T_H$ ) were calculated at the same time through the refinement of several sets of potentiometric data by SUPERQUAD without introducing into the calculations the liquid-junction potentials ( $A_j$  and  $B_j$ ) as shown in previous papers.<sup>13,21</sup> At the end of this refinement the maximum variation in the quantities  $T_L, T_H$  with respect to the initial values was 2.62, 1.19%. There is a need to be able to treat data relating to substances for which only a few milligrams are available, making purification difficult (see ref. 24). GAUSS Z was used to refine  $\beta_{0q1}$  starting from the same experimental data. The calculated protonation and formation constants ( $\log \beta_{pq}$ ) of the ligand are given in Table 2. In the normal aqueous titration range, the fully protonated form of *N*-hydroxy-D-asparagine ( $H_3L^+$ ) can liberate three protons, one from the carboxylic group (COOH) [ $H^1$ ,  $\log K_3^H = 2.18(1)$ ], one from the OH group of the hydroxamic moiety (NHOH) [ $H^2$ ,  $\log K_2^H = 8.15(1)$ ], and one from the protonated amino group ( $NH_3^+$ ) [ $H^3$ ,  $\log K_1^H = 9.37(1)$ ].

These show buffering behaviour in the pH range 2.24—10.50. All the protonation constants calculated by both computer methods agree closely (Table 2). The influence of the  $\alpha$ -amino group in aminohydroxamic acids on the acidic character of the OH group [ $\log K_2^H = 7.48(1)$  for glycinehydroxamic acid (aha),<sup>13</sup> 7.19(2) for L- $\alpha$ -alaninehydroxamic acid (ahpr),<sup>26</sup> 7.34(1) for DL-norvalinehydroxamic acid (ahp),<sup>13</sup> 7.07(1) for L-histidinehydroxamic acid (ahip);<sup>21</sup>  $\log K_3^H = 6.96(1)$  for L-tyrosinehydroxamic acid (ahhpp);<sup>27</sup>  $\log K_2^H = 7.38(1)$  for



DL-norleucinehydroxamic acid (ahhe),<sup>28</sup> 7.04(1) for DL-tryptophanhydroxamic acid (ahinp),<sup>28</sup> 8.15(1) for *N*-hydroxy-D-asparagine (hasn);  $\log K_3^H = 6.77(1)$  for DL-serinehydroxamic acid (adhp);<sup>29</sup> and  $\log K_2^H = 6.89(1)$  for DL-phenylalaninehydroxamic acid (ahpp)<sup>29</sup>]\* can be compared with those of some alkylhydroxamic acids ( $\log K_1^H = 9.56$  for propionohydroxamic acid<sup>30</sup> and  $\log K_1^H = 9.34$  for acetohydroxamic acid<sup>31</sup> etc.). This increase in acidic character (decrease in protonation constant of NHOH group) takes place in the order hasn < aha < ahhe < ahp < ahip < ahinp < ahhpp < ahpp < adhp. Likewise the replacement of a NHOH group for the carboxyl OH group in aminohydroxamic acids lowers the protonation constant of the  $\alpha$ -amino group as compared to the analogous protonation constant of the corresponding  $\alpha$ -amino acids due to the electron-withdrawing effect of the NHOH group [ $\log K_1^H = 9.10(1)$  for glycinehydroxamic acid,<sup>13</sup> 9.54(1) for glycine,<sup>32</sup> 9.13(1) for DL-norvalinehydroxamic acid,<sup>13</sup> 9.68(3) for DL-norvaline,<sup>33</sup> 8.94(1) for L-histidinehydroxamic acid,<sup>21</sup> 9.17 for histidine;<sup>34</sup>  $\log K_2^H = 8.92(1)$  for L-tyrosinehydroxamic acid,<sup>27</sup> 9.07(5) for L-tyrosine;<sup>33</sup>  $\log K_1^H = 9.17(1)$  for DL-norleucinehydroxamic acid,<sup>28</sup> 9.67(3) for DL-norleucine,<sup>33</sup> 9.09(1) for DL-tryptophanhydroxamic acid,<sup>28</sup> 9.49 for DL-tryptophan,<sup>32</sup> 9.15(1) for L- $\alpha$ -alaninehydroxamic acid,<sup>26</sup> 9.66 for L-alanine,<sup>32</sup> 9.37(1) for *N*-hydroxy-D-asparagine, 9.87 for D-aspartic acid, 9.01(1) for DL-phenylalaninehydroxamic acid,<sup>29</sup> 9.11(2) for DL-phenylalanine;<sup>32</sup>  $\log K_2^H = 8.90(1)$  for DL-serinehydroxamic acid<sup>29</sup> and 9.06 for DL-serine<sup>32</sup>]. Plotting the protonation constant ( $\log K_1^H$ ) of the  $\alpha$ -amino group for some aminohydroxamic acids against  $\log K_1^H$  for the  $\alpha$ -amino group of the corresponding amino acids yields a straight line of positive slope (0.44) (Figure 1) in which the abnormally low tendency for  $NH_3^+$  of hasn to deprotonate is due to the presence of one COOH group in hasn compared to two COOH groups in D-aspartic acid. The variations of  $\log K_2^H$  (protonation constant of NHOH group) against  $\log K_1^H$  (protonation constant of  $\alpha$ -amino group) for all the aminohydroxamic acids examined are analogous to those reported previously.<sup>13,21,27-29</sup>

**Metal(II) Complex Equilibria.**—Starting from several sets of potentiometric data all the protonation constants, except  $\log \beta_{031}$  relevant to the protonation of  $-COO^-$ , were kept constant and the SUPERQUAD program<sup>24</sup> applied to obtain the best-fitting chemical models and refined formation constants ( $\log \beta_{pq}$ ). The results are shown in Table 2. Potentiometric titration curves of the protonated ligand,  $H_3L^+$ , alone or in the presence of  $Co^{2+}$ ,  $Ni^{2+}$ , or  $Cu^{2+}$  are shown in Figure 2. In the presence of metal ions the curves reveal an appreciable complexing capacity in the acidic media, especially for  $Cu^{2+}$ , which takes place before neutralization of  $-COOH$ . Titration of protonated *N*-hydroxy-D-asparagine ( $H_3L^+$ , 0.012 mol  $dm^{-3}$ ) in the

\* Abbreviations: aha = 2-amino-*N*-hydroxyacetamide, ahpr = 2-amino-*N*-hydroxypropanamide, ahp = 2-amino-*N*-hydroxypentamide, ahip =  $\alpha$ -amino-*N*-hydroxy-1*H*-imidazole-4-propanamide, ahhe = 2-amino-*N*-hydroxyhexanamide, ahinp =  $\alpha$ -amino-*N*-hydroxy-1*H*-indole-3-propanamide, ahhpp = 2-amino-*N*-hydroxy-3-(*p*-hydroxyphenyl)propanamide, ahpp = 2-amino-*N*-hydroxy-3-phenylpropanamide, adhp = 2-amino-*N*,3-dihydroxypropanamide.

**Table 2.** Cumulative and stepwise protonation complex-formation constants of *N*-hydroxy-D-asparagine (hasn) with bivalent metal ions at 25 °C and  $I = 0.5 \text{ mol dm}^{-3}$  (KCl). Standard deviations ( $\sigma$  values) are given in parentheses

	SUPERQUAD				GAUSS Z
	H <sup>+</sup>	Co <sup>II</sup>	Ni <sup>II</sup>	Cu <sup>II</sup>	H <sup>+</sup>
log $\beta_{011}$	9.37(1)				9.37(1)
log $\beta_{021}$	17.52(1)				17.51(1)
log $\beta_{031}$	19.70(1)	19.89(1)	19.93(2)	19.64(1)	19.69(1)
log $K_2^{\text{H}^a}$	8.15(1) <sup>b</sup>				8.13(1)
log $K_3^{\text{H}}$	2.18(1)				2.18(1)
log $\beta_{111}$		13.91(2)	14.25(3)		
log $\beta_{101}$		7.56(2)	8.38(3)	12.60(1)	
log $\beta_{203}$		23.43(3)	25.78(4)	37.45(5)	
log $\beta_{304}$				53.43(9)	
log $\beta_{102}$		12.86(3)	14.73(6)	19.07(4)	
log $\beta_{1-12}$		2.46(7)		9.08(4)	
$Z^c$	221	309	272	206	221
$U$	$1.927 \times 10^2$	$2.432 \times 10^3$	$3.170 \times 10^3$	$9.99 \times 10^2$	$7.530 \times 10^{-2d}$
$\chi^2^e$	9.33	6.68	6.35	23.59	
$\sigma^f$	0.96	2.86	3.53	2.23	$3.454 \times 10^{-4g}$

<sup>a</sup>  $\log K_n^{\text{H}} = \log \beta_{0n1} - \log \beta_{0n-11}$ . <sup>b</sup>  $\sigma(\log K_n^{\text{H}}) = \{[\sigma^2(\log \beta_{0n1}) + \sigma^2(\log \beta_{0n-11})]/2\}^{1/2}$ . <sup>c</sup> Total number of experimental data points used in the refinement. <sup>d</sup>  $U = \sum_{i=1}^Z (\bar{n}_i^{\text{calc.}} - \bar{n}_i^{\text{obs.}})^2$ , where  $n_i$  is the observed (obs.) or calculated (calc.) average number of hydrogen ions bound to each central ligand molecule. <sup>e</sup> Observed  $\chi^2$ ; calculated value (6, 0.95) should be 12.6, where 6 is the number degrees of freedom and 0.95 is the confidence coefficient in the  $\chi^2$  distribution. <sup>f</sup>  $\sigma = \sqrt{\sum_{i=1}^Z w_i (E_i^{\text{obs.}} - E_i^{\text{calc.}})^2 / (Z - m)}$ , where  $m$  is the number of parameters to be refined. <sup>g</sup>  $\sigma^2 = \sum_{i=1}^Z (\bar{n}_i^{\text{calc.}} - \bar{n}_i^{\text{obs.}})^2 / (Z - m)$ .

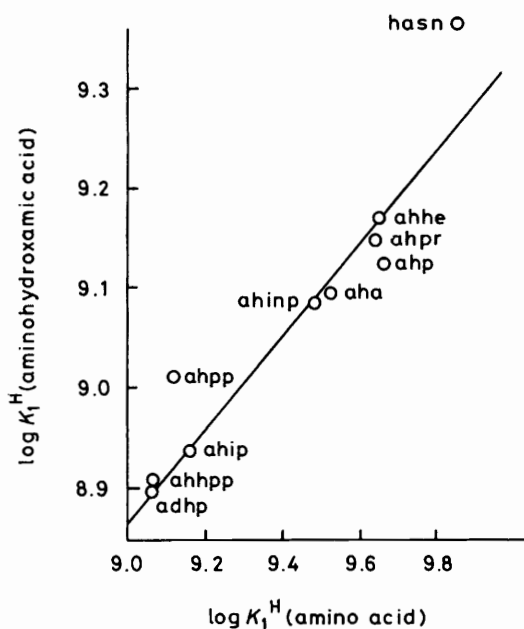


**Figure 1.** Relationship between  $\log K_1^{\text{H}}$  (protonation constant of  $\alpha$ -amino group in aminohydroxamic acids) and  $\log K_1^{\text{H}}$  (protonation constant of  $\alpha$ -amino group of the corresponding amino acids). The line drawn was obtained from a linear least-squares analysis of all the data ( $y = 4.926 + 0.44x$ )

presence of copper(II) ions ( $0.004 \text{ mol dm}^{-3}$ ) shows two inflection points corresponding to the release of 4.5 and 6 protons per copper respectively, which can be related to reactions (5) and (6).



The shapes of the curves clearly show that different types of reaction are occurring involving the formation of simple mononuclear chelates,  $[\text{ML}]$  and  $[\text{ML}_2]$ , as well as various polynuclear,  $[\text{M}_3\text{L}_4]$  and  $[\text{M}_2\text{L}_3]$ , monohydrogen,  $[\text{MHL}]$ , or hydrolyzed,  $[\text{M}(\text{OH})\text{L}_2]$ ,\* species. The titration curves for  $\text{Ni}^{2+}$  and  $\text{Co}^{2+}$  differed in shape to those of  $\text{Cu}^{2+}$ .

Experimental data ( $v, E$ ) were processed initially by NBAR<sup>23</sup> to obtain formation curves [ $\bar{n}$  versus pL, equations (7) and (8)].

$\bar{n} =$

$$\frac{[\text{L}]_{\text{T}} - [\text{L}^{2-}](1 + [\text{H}^+]\beta_{011} + [\text{H}^+]^2\beta_{021} + [\text{H}^+]^3\beta_{031})}{[\text{M}]_{\text{T}}} \quad (7)$$

$$[\text{L}^{2-}] = \frac{[\text{H}]_{\text{T}} - \frac{v \cdot c_{\text{KOH}}}{V_0} + [\text{OH}^-] - [\text{H}^+]}{\beta_{011}[\text{H}^+] + 2\beta_{021}[\text{H}^+]^2 + 3\beta_{031}[\text{H}^+]^3} \quad (8)$$

This strategy facilitated the search for not only mononuclear binary complexes but also polynuclear species, particularly in the copper(II)-hasn system.

Plots of  $\bar{n}$  against  $-\log[\text{L}^{2-}]$  from some potentiometric titrations (runs 6, 7, and 8, Table 1) of copper(II)-hasn mixtures are shown in Figure 3. That the formation curves are not superimposable indicates the presence of polynuclear complexes. On the other hand, the curves are not parallel with a spacing,  $\Delta \log[\text{L}^{2-}]$ , proportional to  $\Delta \log[\text{M}]_{\text{T}}$ , so the system does not contain predominantly a 'core plus links' series of complexes.<sup>35,36</sup> That the spacing between the curves in different systems decreases as the metal ion concentration is reduced suggests that mononuclear complexes are the major species in the more dilute solutions and that the curves are converging towards Biedermann and Sillén's 'mononuclear wall'.<sup>37,38</sup> The curves (Figure 3) intersect at the point  $\bar{n} = 1.33$ , pL = 9.5.

\*  $\beta_{1-12}$ , equilibrium constant for the reaction:  $\text{M}^{2+} + 2\text{L}^{2-} + \text{H}_2\text{O} \rightleftharpoons [\text{M}(\text{OH})\text{L}_2]^{3-} + \text{H}^+$ .

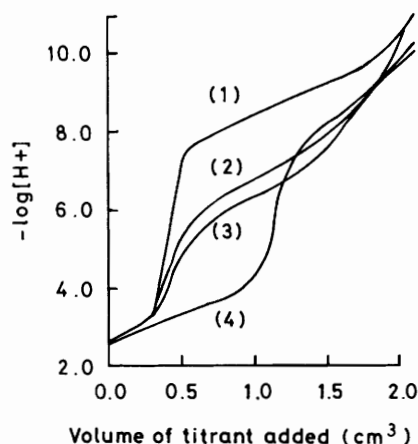


**Figure 2.** Titration curves of pH as a function of the volume of KOH added, calculated by the HALTAFALL program and using a Calcomp 936 PLOTTER. Initial concentration of solutions:  $c_H = 0.030$ ,  $c_L = 0.012$ ,  $c_M = 0.004$ ,  $c_{KOH} = 0.375 \text{ mol dm}^{-3}$ ,  $V_0 = 25.0 \text{ cm}^3$ . Curves: (1) hasn, (2)  $\text{Co}^{2+}$ -hasn, (3)  $\text{Ni}^{2+}$ -hasn, and (4)  $\text{Cu}^{2+}$ -hasn

According to various authors,<sup>39-41</sup> the existence of a cross-over point signifies an equilibrium between two polynuclear species ( $[\text{Cu}_3\text{L}_4]^{2-}$ ,  $[\text{Cu}_2\text{L}_3]^{2-}$ ), coexisting with the mononuclear complexes,  $[\text{CuL}]$  or  $[\text{CuL}_2]^{2-}$ . Using the formation constants given in Table 2 and the protonation constants of the ligand under the same experimental conditions, the percentage of each complex involving  $\text{H}^+$  or  $\text{OH}^-$ , metal ion, and ligand has been evaluated by the HALTAFALL program.<sup>42</sup> Figure 4 illustrates typical distribution diagrams.

The spectrophotometric study was carried out on a series of solutions, containing hasn and copper(II), at concentrations and pH values selected from those employed in the potentiometric experiments. Since the literature on similar systems is very poor, the qualitative interpretation was carried out by comparison with the well known spectra of  $\text{Cu}^{\text{II}}$ -aminohydroxamic acids and -amino acids. The absorption spectra (Figure 5) of the  $\text{Cu}^{\text{II}}$ -hasn system exhibit, in general, approximately the same changes with increasing pH to those observed for the  $\text{Cu}^{\text{II}}$ -aminohydroxamic acid system.<sup>13,21,26-29,43</sup> Some differences are observed in the energy of the characteristic absorption maxima. The complex formation begins at low pH (Figure 4, *ca.* 2.7). When the pH is increased a high combined hypochromic-hyperchromic effect is observed in the range 615–746 nm. The increase in absorption of the broad spectrum near the i.r. region and the shift towards smaller wavelengths (visible region) [746.0 for (6), 684.0 for (5), 646.0 for (4), 625.0 for (3), 618.0 for (2), 615.0 nm for (1), Figure 5(a)] of the same band with increasing pH indicates greater complexation, and above pH 9.0 [Figure 5(b), (1)] both  $\lambda_{\text{max}}$  and  $\epsilon_{\text{max}}$  do not change any further, consistent with formation of the  $[\text{Cu}(\text{OH})\text{L}_2]^{3-}$  species which predominates in this range. At pH 5.6 the maximum occurring at 615 nm corresponds to the greatest concentration of the polynuclear complex  $[\text{Cu}_3\text{L}_4]^{2-}$  [Figure 4(a)].

Copper, in its various roles in biological systems, displays differing spectroscopic and chemical properties presumably because of the differing ligand environments and co-ordination numbers. The bonding mode in the  $[\text{ML}]$  and  $[\text{ML}_2]^{2-}$  etc. complexes of aminohydroxamic acids is almost certainly not glycine-like, where the metal ion is bound through the carboxylate and  $\alpha$ -amino groups only. The much higher stability of the 1:1 and 1:2 complexes of hasn and other aminohydroxamic acids<sup>13,21,26-28</sup> with various metal ions compared with the same complexes of the corresponding amino acids (*e.g.* D-aspartic acid, glycine, histidine, DL-norvaline, DL-

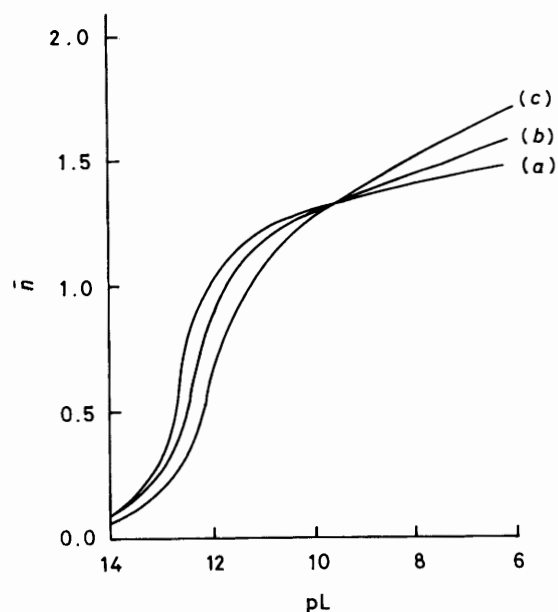


**Figure 3.** Formation curves ( $\bar{n}$  versus pL) for potentiometric titrations [runs 6(a), 7(b), and 8(c), Table 1] of the  $\text{Cu}^{2+}$ -hasn system

tryptophan, L-tyrosine, DL-norleucine, etc.) can be attributed to co-ordination *via* the nitrogen atom of the  $\alpha$ -amino group and the nitrogen of the  $\text{NHO}^-$  group. Following Billo<sup>44</sup> and other workers<sup>26,43</sup> the ligand-field contributions of all the donor groups [ $\nu_{\text{N}(\text{amino})}$  4 540,  $\nu_{\text{N}(\text{hydroxamate})}$  4 650,  $\nu_{\text{O}(\text{carboxylate})}$  3 420, and  $\nu_{\text{O}(\text{H}_2\text{O}, \text{OH}^-)}$  3 010  $\text{cm}^{-1}$ ] in  $[\text{Cu}_3\text{L}_4]^{2-}$  (observed  $\nu_{\text{max}}$  at 16 300, 615 nm) were employed to predict *d-d* transition energies and identify the co-ordination sites (I). By using the 'rule of average environment'<sup>44</sup> the result (calculated  $\nu_{\text{max}}$  at 16 530  $\text{cm}^{-1}$ ) indicates that, at least for the donor atoms considered here,  $\nu_{\text{max}}$  of a square-planar copper(II) complex, in which the nitrogen atoms occupy the four co-ordination sites (partially filled by oxygen atoms) with *trans* geometry [(I)–(III)], can be predicted with good accuracy. For the dinuclear complex  $[\text{Cu}_2\text{L}_3]^{2-}$  (II) ( $\nu_{\text{max}}$  at *ca.* 605 nm), which reaches a maximum concentration of 89.8% total copper at pH 7.3 [Figure 4(a)], co-ordination of three aminohydroxamate moieties to two copper ions *via* the nitrogens of the amino and hydroxamate groups would contribute 9 180  $\text{cm}^{-1}$  to the *d-d* transition energies. The two remaining groups would therefore have to contribute 3 420 [ $\nu_{\text{O}(\text{carboxylate})}$ ] and 3 010  $\text{cm}^{-1}$  [ $\nu_{\text{O}(\text{H}_2\text{O})}$ ], in order to approach the observed  $\nu_{\text{max}}$  (*ca.* 16 500  $\text{cm}^{-1}$ ).

The structure of  $[\text{CuL}]$  has not been reported, but it is reasonable to assume it will be similar to that proposed for  $[\text{CuL}_2]^{2-}$  (III), in which two positions are occupied by  $\text{H}_2\text{O}$  molecules. The present ligand as well as various aminohydroxamic acids (*e.g.* aha,<sup>13,43</sup> ahp,<sup>13</sup> adhp,<sup>29</sup> ahpr,<sup>26</sup> ahhe<sup>28</sup> etc.) and amines (*e.g.*  $\text{NH}_3$  or  $\text{H}_2\text{NCH}_2\text{CH}_2\text{NH}_2$ ) produces a stronger ligand field than  $[\text{Cu}(\text{H}_2\text{O})_6]^{2+}$ , which causes the absorption band to move from the far red to the middle of the red region of the spectrum. Therefore, I suggest a  $d_{xy}$  ground state for the copper(II)-hasn system with square-planar geometry. A maximum near 605–615 nm, in which square-planar  $\text{Cu}^{2+}$  complexes showing a marked red shift in aqueous solution are sensitive to axial perturbation by co-ordinated  $\text{H}_2\text{O}$  molecules, is tentatively assigned to  $d_{xy}-d_{x^2-y^2}$ .

The characteristic isosbestic point seen at 763 nm is associated with equilibria between polynuclear ( $[\text{Cu}_3\text{L}_4]^{2-}$ ,  $[\text{Cu}_2\text{L}_3]^{2-}$ ) and mononuclear ( $[\text{CuL}]$ ,  $[\text{CuL}_2]^{2-}$ ) complexes. The only colour variation observed for the copper(II)-hasn

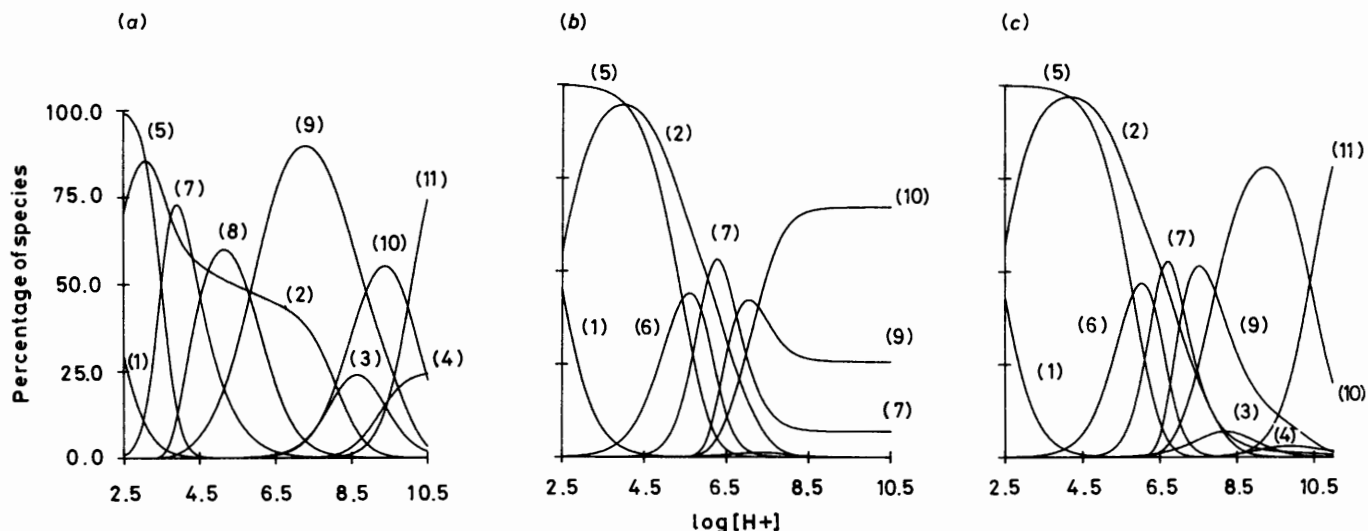


**Figure 4.** Typical distribution diagrams for  $M^{2+}$ -hasn systems. The percentage of each species has been calculated from the data for a hypothetical solution of metal ions [ $0.0041$  ( $Cu^{2+}$ ),  $0.00588$  ( $Ni^{2+}$ ), or  $0.0092$  ( $Co^{2+}$ )  $mol\ dm^{-3}$ ] and hasn [ $0.011$  (a),  $0.0106$  (b), or  $0.00455$  (c)  $mol\ dm^{-3}$ ] by the HALTAFALL program. The concentrations of the species not containing metal were calculated as percentages of the total ligand, those containing metal as percentages of the total metal: (a)  $Cu^{2+}$ -hasn, (b)  $Ni^{2+}$ -hasn, (c)  $Co^{2+}$ -hasn; (1)  $H_3L^+$ , (2)  $H_2L$ , (3)  $HL^-$ , (4)  $L^{2-}$ , (5)  $M^{2+}$ , (6)  $[MHL]^+$ , (7)  $[ML]$ , (8)  $[M_3L_4]^{2-}$ , (9)  $[M_2L_3]^{2-}$ , (10)  $[ML_2]^{2-}$ , and (11)  $[M(OH)L_2]^{3-}$ .

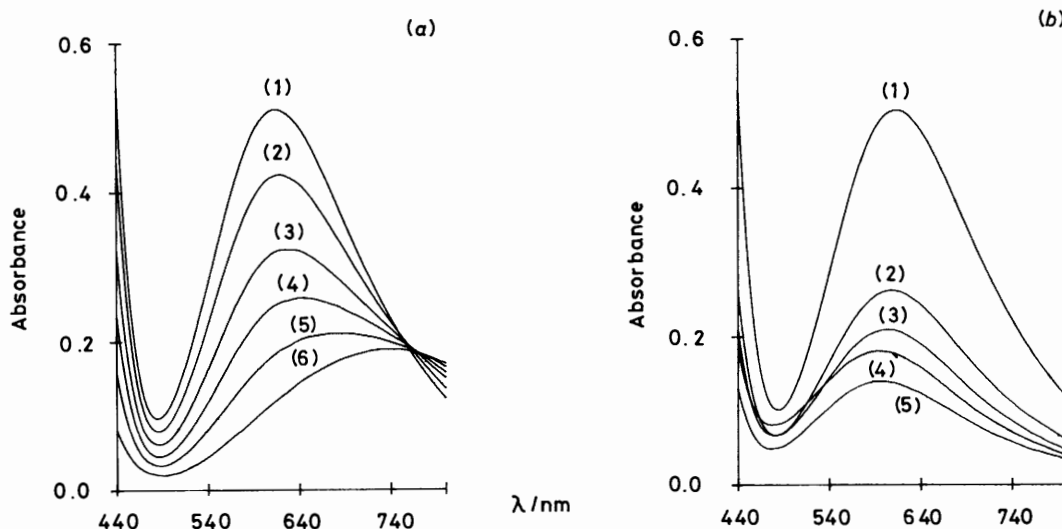
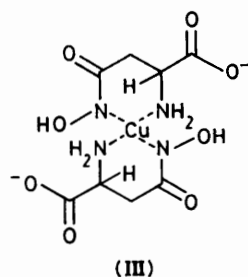
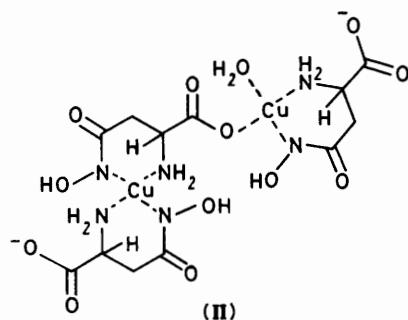
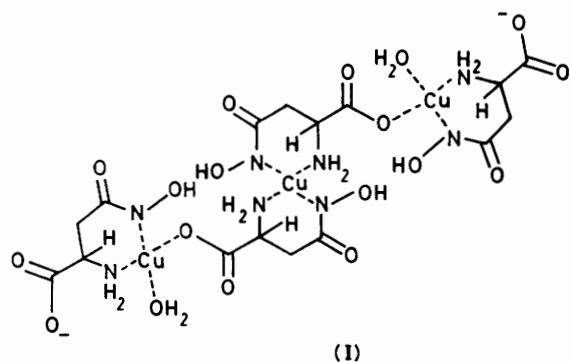


**Figure 5.** Plots of experimental absorbance data versus wavelength for some solutions of  $Cu^{2+}$ -hasn using the program VISION and the Calcomp 936 PLOTTER. (a) (1) pH 5.60,  $c_L = 7.101 \times 10^{-3}$ ,  $c_M = 7.252 \times 10^{-3}$ ; (2) pH 3.88,  $c_L = 7.018 \times 10^{-3}$ ,  $c_M = 7.167 \times 10^{-3}$ ; (3) pH 3.63,  $c_L = 6.937 \times 10^{-3}$ ,  $c_M = 7.084 \times 10^{-3}$ ; (4) pH 3.51,  $c_L = 6.883 \times 10^{-3}$ ,  $c_M = 7.030 \times 10^{-3}$ ; (5) pH 3.40,  $c_L = 6.831 \times 10^{-3}$ ,  $c_M = 6.976 \times 10^{-3}$ ; (6) pH 3.30,  $c_L = 6.780 \times 10^{-3}$ ,  $c_M = 6.923 \times 10^{-3}$   $mol\ dm^{-3}$ . (b) (1) pH 11.12,  $c_L = 7.187 \times 10^{-3}$ ,  $c_M = 7.339 \times 10^{-3}$ ; (2) pH 11.27,  $c_L = 7.252 \times 10^{-3}$ ,  $c_M = 3.703 \times 10^{-3}$ ; (3) pH 11.42,  $c_L = 8.340 \times 10^{-3}$ ,  $c_M = 2.920 \times 10^{-3}$ ; (4) pH 11.10,  $c_L = 9.087 \times 10^{-3}$ ,  $c_M = 2.381 \times 10^{-3}$ ; (5) pH 10.92,  $c_L = 8.617 \times 10^{-3}$ ,  $c_M = 1.886 \times 10^{-3}$   $mol\ dm^{-3}$ .

system is from green-blue in acid solution, to blue-green in slightly acid solution to blue in neutral and alkaline media. The increase in absorption and the slight shift to longer wavelengths [596–615 nm, Figure 5(b)] from pH 9.0 to 11.4 with increase in copper(II) concentration correspond to the predominance of  $[CuL_2]^{2-}$  and  $[Cu(OH)L_2]^{3-}$  in this pH range. The titration curves for  $Ni^{2+}$  and  $Co^{2+}$  had shapes different to those of  $Cu^{2+}$  (Figure 2). The refinement converged satisfactorily when the only species present were  $[CoHL]^+$ ,  $[CoL]$ ,  $[Co_2L_3]^{2-}$ ,  $[CoL_2]^{2-}$ , and  $[Co(OH)L_2]^{3-}$  for  $Co^{2+}$  and  $[NiHL]^+$ ,  $[NiL]$ ,  $[Ni_2L_3]^{2-}$ , and  $[NiL_2]^{2-}$  for  $Ni^{2+}$ . The relative importance of the various species in each pH range is shown by the

distribution diagrams for hasn with  $Ni^{2+}$  and  $Co^{2+}$  [Figure 4(b) and (c)]. In weakly acidic solution, bonding through the oxygen of the carboxylate group and the  $\alpha$ -amino nitrogen is probably favoured with the OH proton of the NHOH group not being involved, resulting in the formation of  $[MHL]^+$  [maximum concentration of 43.8% total metal at pH 5.4 for  $Ni^{2+}$ , 47.0% at pH 6.1 for  $Co^{2+}$ , Figure 4]. At intermediate pH,  $[ML]$  reaches a maximum concentration of 72.2% total copper at pH 3.9, 53.4% total nickel at pH 6.5, and 52.8% total cobalt at pH 6.7. At pH ca. 9.0 the hydroxamic acid functional groups of hasn are completely ionized and the predominant species is  $[CuL_2]^{2-}$  which reaches a peak of 54.8% at pH 9.4 ( $[NiL_2]^{2-}$ ,



67.0% at pH 9.0;  $[\text{CoL}_2]^{2-}$ , 78.1% at pH 9.3). In the physiological pH range (6.7–7.3)  $[\text{Cu}_2\text{L}_3]^{2-}$  accounts for over 89.8% of the total metal (97.8% for species  $[\text{Ni}_2\text{L}_3]^{2-}$ ,  $[\text{NiL}]$ , and  $[\text{NiL}_2]^{2-}$ ; 88.7% for species  $[\text{Co}_2\text{L}_3]^{2-}$ ,  $[\text{CoL}]$ , and  $[\text{CoL}_2]^{2-}$ ). It is reasonable to assume that for the  $\text{Ni}^{\text{II}}$  complexes co-ordination by the aminohydroxamic acid side of the molecule, after deprotonation of  $-\text{COOH}$  [Figure 2,(3)], easily occurs *via* the nitrogen atom of the  $-\text{CONHOH}$  group rather than through the oxygen atom, as previously described.<sup>1,3,21,27</sup> For the majority of cases the larger  $\log \beta_{101}$ ,  $\log \beta_{102}$ , and  $\log K_2$  values for hasn compared to those for aha, ahpr, and ahhe presumably reflect the greater basicities of its  $\text{NHOH}$  ( $\log K_2^{\text{H}}$ ) and  $\alpha$ -amino groups ( $\log K_1^{\text{H}}$ ). The Irving-Williams order is followed for complexes  $[\text{ML}]$ ,  $[\text{ML}_2]^{2-}$ , and  $[\text{MHL}]^+$ . The  $\text{M}^{\text{II}}$ -hasn system can therefore probably satisfy different criteria for biological activities and analytical roles, strongly indicating  $\text{M}^{\text{II}}$ -hasn complexes as suitable sources of metal ions as trace elements essential in animal nutrition. The results show that, at least in the  $\text{M}^{\text{II}}$ -hasn system at physiological pH, the assumption of an unco-ordinated  $\alpha$ -amino group is incorrect.

### Acknowledgements

Financial support in part by the Ministero della Pubblica Istruzione, Rome, and by the National Research Council of Italy (C.N.R.) is gratefully acknowledged. I am greatly indebted

to Professor P. Gans, A. Vacca, and A. Sabatini the authors of the program SUPERQUAD for their generous support.

### References

- W. N. Fishbein, C. L. Streeter, and J. E. Daly, *J. Pharmacol. Exp. Ther.*, 1973, **186**, 173.
- N. E. Dixon, R. L. Blakely, and B. Zerner, *Can. J. Biochem.*, 1980, **58**, 1323.
- H. Maehr, *Pure Appl. Chem.*, 1971, **28**, 603.
- J. B. Neilands, *Struct. Bonding (Berlin)*, 1966, **1**, 59.
- J. B. Neilands, 'Bioinorganic Chemistry II,' ed. K. N. Raymond, Advances in Chemistry Series, No. 162, Washington D.C., 1977, p.3.
- J. B. Neilands, *J. Bacteriol.*, 1976, **126**, 823.
- R. T. Coutts, *Can. J. Pharm. Sci.*, 1967, **2**, 27.
- R. T. Coutts, *Can. J. Pharm. Sci.*, 1967, **2**, 1.
- D. A. Brown, A. L. Roche, T. A. Pakkanen, T. T. Pakkanen, and K. Smolander, *J. Chem. Soc., Chem. Commun.*, 1982, 676.
- D. A. Brown and M. V. Chidambaram, 'Iron-Containing Drugs,' in 'Metal Ions in Biological Systems,' ed. H. Sigel, Marcel Dekker, New York, 1982, vol. 14, p. 125.
- G. W. Bates and J. Wernicke, *J. Biol. Chem.*, 1971, **246**, 3679.
- W. F. Anderson and M. C. Hiller, DHEW Publication No. (NIH)(U.S.), 1976, p. 994.
- E. Loporati, *J. Chem. Soc., Dalton Trans.*, 1986, 2587.
- G. Schwarzenbach and K. Schwarzenbach, *Helv. Chim. Acta*, 1963, **46**, 1930.
- R. G. Motekaitis, I. Murase, and A. E. Martell, *J. Coord. Chem.*, 1971, **1**, 77.
- Y. K. Agrawal, *Bull. Soc. Chim. Belg.*, 1980, **89**, 166.
- F. Bigoli, E. Loporati, and M. A. Pellinghelli, *J. Chem. Soc., Dalton Trans.*, 1981, 1961.
- E. Loporati, *J. Chem. Soc., Dalton Trans.*, 1985, 199.
- F. Bigoli, E. Loporati, and M. A. Pellinghelli, *J. Chem. Soc., Dalton Trans.*, 1981, 1531.
- E. Loporati, *Anal. Chim. Acta*, 1985, **170**, 287.
- E. Loporati, *J. Chem. Soc., Dalton Trans.*, 1987, 435.
- G. Gran, *Analyst (London)*, 1952, **77**, 661.
- H. S. Harris and R. S. Tobias, *Inorg. Chem.*, 1969, **8**, 2259.
- P. Gans, A. Sabatini, and A. Vacca, *J. Chem. Soc., Dalton Trans.*, 1985, 1195.
- R. S. Tobias and M. Yasuda, *Inorg. Chem.*, 1963, **2**, 1307.
- B. Kurzak, K. Kurzak, and J. Jezierska, *Inorg. Chim. Acta*, 1986, **125**, 77.
- E. Loporati, *J. Chem. Soc., Dalton Trans.*, 1987, 1409.
- E. Loporati, *J. Chem. Soc., Dalton Trans.*, 1987, in the press.
- E. Loporati, *J. Chem. Soc., Dalton Trans.*, submitted for publication.
- D. A. Brown and A. L. Roche, *Inorg. Chem.*, 1983, **22**, 2199.
- D. A. Brown, M. V. Chidambaram, J. J. Clarke, and D. M. McAleese, *Bioinorg. Chem.*, 1978, 225.
- A. E. Martell and R. M. Smith, 'Critical Stability Constants,' Plenum Press, New York and London, 1974, vol.1.
- A. Gergely, I. Sovago, I. Nagypal, and R. Kiraly, *Inorg. Chim. Acta*, 1972, **6**, 435.
- A. C. Andrews and D. M. Zebolsky, *J. Chem. Soc.*, 1965, 742.
- L. G. Sillén, *Acta Chem. Scand.*, 1954, **8**, 299.
- F. J. C. Rossotti and H. R. Rossotti, 'The Determination of Stability Constants,' McGraw-Hill, New York, 1961, p. 355.
- G. Biedermann and L. G. Sillén, *Acta Chem. Scand.*, 1956, **10**, 1011.
- D. D. Perrin and I. G. Sayce, *J. Chem. Soc. A*, 1967, 82.
- G. Carpeni, *Bull. Soc. Chim. Fr.*, 1948, 629.
- G. Carpeni, *Compt. Rend.*, 1940, **226**, 807.
- N. Ingri, G. Lagerström, M. Frydman, and L. G. Sillén, *Acta Chem. Scand.*, 1957, **11**, 1034.
- N. Ingri, W. Kakalovicz, L. G. Sillén, and B. Warnqvist, *Talanta*, 1967, **14**, 1261.
- E. B. Paniago and S. Carvalho, *Inorg. Chim. Acta*, 1984, **92**, 253.
- E. J. Billo, *Inorg. Nucl. Chem. Lett.*, 1974, **10**, 613.

Received 30th April 1987; Paper 7/773